2DOF flexible Link Manipulator Model Simulation Inventor: Finite Element Analysis with varying payloads at the tip.

XS Nyathi[1] and FK Tekweme[1]

[1] Department of Mechanical and Industrial Engineering, University of Johannesburg, 55 Beit St, Doornfontein, Johannesburg 2028, South Africa

201461366@student.uj.ac.za, fktekweme@uj.ac.za

Abstract. Robots are used to assist human beings in various applications. There is a need to improve the performance of robot structures by cutting cost and to provide light-weighted material systems. An area of flexible link manipulator has gained more interest from researchers in robotics. When compared with rigid-link manipulators, flexible manipulators are easy to manoeuvre, high-speed performance and higher payload-to-weight ratio. It has been noted that in previous and recent years' experiments were proposed in analysing tip deflection. In this paper a model of 2DOF Flexible Link Manipulator (FLM) in a cantilever configuration, it has been designed from a lightweight material. The aim is to assess the stability of the FLM model with a set of varying payloads attached at the tip as to what will be the maximum load it can withstand. The Inventor design tool was used to simulate the loading procedures, which assisted with Finite element analysis. Results are compared against the allowable maximum deflection limit of cantilever configuration. Results on how the model deflects are produced with the safety factor at each loaded condition and numerical results of maximum deflection produced by the set of varying loads were compared with the FEA results. And based on the results assessed, conclusions are made with a set of safety factor and how the light weighted design is advantageous in the industry to improve safety and performance.

Keywords: Flexible manipulator, model simulation, light material, FEA, deflection, payload

1. Introduction

Engineers and researchers have focussed on modelling a flexible manipulator, and so far with controlling the vibrations occurring when the model has moved and stopped, mostly conducted with theoretical models. Amongst other uses, this new area of flexible link manipulator has gained interest from researchers in robotics. When Compared with rigid-link robotic structures, flexible manipulators are easy to manoeuvre, high-speed performance and higher payload-to-weight ratio (Agee, et al., 2014). And the two-link flexible manipulator poses the rigid and flexible type of motions because of their mechanical flexibility, they are lightweight, (Sahu, et al., 2017) explains that they are easy to transport as they are compared to rigid robot arms which in the way they are structured tend to be inefficient and they have to carry less weight. Balancing the flexibility and the weight of the links in these flexible manipulators is necessary (Rezaei & Shafei, 2019).

Flexible link manipulators (FLM) are constructed like human arms some with more joints. They are continuously replacing rigid manipulators (Yu, et al., 2015) in the industry due to fewer energy demands when operating FLM. The controlling of a flexible manipulator, it is performed by actuating the joints to move at a certain speed

(Bhandari & Kalaichelvi, 2017) or a specified angle. So, in this paper, the flexible link manipulator is tested before it is actuated to what load it can carry.

Nominal payloads of $0{,}157kg$ and $0.457\ kg$ were used in a study conducted by (Pradhan & Subudhi, 2011) for an actuated flexible manipulator and in fuzzy learning-based adaptive control same payloads were applied in another study by (Pradhan & Subudh, 2013). And the model used was made of steel beams a weight ratio can come to play to assess the specific payloads to be used in this paper because the model is designed from aluminium material. A nominal payload load of 0.145kg and later on of 0.3kg was used in MATLAB simulation for a two-link flexible manipulator with a link of 0.202m and 0.2018m in length (Lochan, et al., 2018). Set of varying payloads of 0 up to 100 grams were used in a simulation of the dynamic model of a Two link flexible manipulator by (Ahmad, et al., 2008). (Afolabi, et al., 2019) stated that it is very crucial to determine the cause of failure machine component, this is to reduce risks and improvement of component performance. Inventor software was used (Afolabi, et al., 2019) to simulate a component with Finite Element Analysis (FEA) to get stresses and safety factor. ANSYS software was used by (Pedram & Khedmati, 2014) to conduct finite element investigations.

The use of Inventor software showed that Von messes stresses, the first principal and third principal stresses can be attained with finite element analysis when (Mustika, et al., 2020) conducted a study on power screw fatigue failure load. The importance of the finite element analysis is to display the mechanical performance of the composite structures specific to the actual model (Durbaca, et al., 2019). The use of finite element analysis was adopted by (Afolabi, et al., 2019) using Inventor software and solid works. In a study conducted by (Zuyev, 2015) a payload was considered clamped at the tip of a single link manipulator, it was explained that in practical models payloads are mostly ignored. So in this paper, the application of payload is shifted to a two-link flexible manipulator model designed using Autodesk Inventor software.

It is considered for the design, two conditions: robustness and stability of the Flexible link manipulator model. In this work of modelling a flexible link manipulator, the similar idea of having FLM with uniform beam links it is adapted. The cross-sectional area of the links are to be uniform and the material properties are considered uniform because the lengths of the links are longer than the sectional length thus considering shear deformation in the vertical direction, but (Ying & Wenkai, 2008) and (Sahu, et al., 2017) considered the elastic deformation in the horizontal direction of actuated FLM. The gravity and the shear deformation influence were ignored in the study conducted by (Gao, et al., 2019) as the motion of the model was considered. Thus, this research focusses on the finite element analysis of the designed two link FLM model unactuated and the effects of gravity it is considered to assess fully the stability of the FLM model. In section 2 the flexible manipulator is described, setting up the loading criteria and deriving of limiting deflection is covered, in section 3 simulations of a set of loading conditions is described with defined parameters and section 4 provides the simulated results and discussions and the paper ends with conclusions in section 5.

2. Model Framework of the two-link flexible Manipulator

2.1. Model Description

The 3-D model was generated as a structural assembly where it contains a support rib (as a cantilever fixed point it is made from mild steel) where the whole model is fixed on. The shoulder joint (stepper motor mounted by thin plates as supports and hooks made from aluminium), Shoulder link (made from aluminium, elbow joint (contains a stepper motor and thin plates as supports) and elbow link (shorter than shoulder link and it is made from aluminium). The designed model is restricted to move in the horizontal axis through 0 to 180 degrees. Figure 1 below gives and overview of the designed model, with its description.

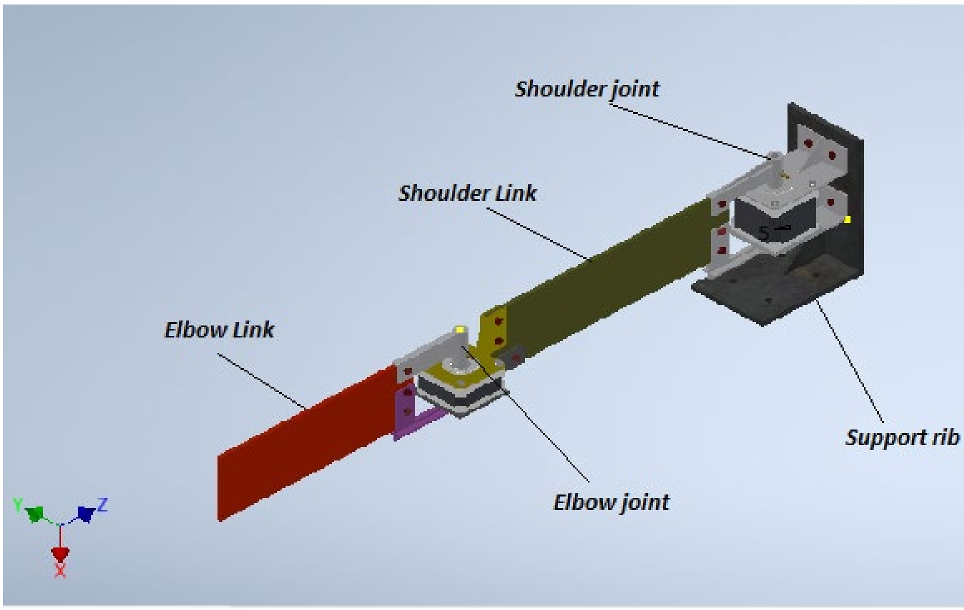

Figure 1:Two-link Flexible manipulator model

With the aid of the Inventor software the physical description of the model is shown in table 1, the whole model is 504 mm long and 106 mm in height, with a total mass of approximately 0.84 kg. In the table the volume of the mdel is provided and the location of gravity.

Table 1: Physical parameters of the Flexible manipulator model

Name	Quantity
Mass	$0,836914\ kg$
Area	$145060\ mm^2$
Volume	$179325\ mm^3$
Centre of Gravity	$x = -0,199655\ mm$
	$y = 0,556929\ mm$
	$z = -74,7881\ mm$
Height	$106\ mm$
Width	$60\ mm$
Length	$504\ mm$

2.2. Cantilever beam configuration and limiting deflection

As the model is in cantilever configuration, execution of some formulae in engineering to determine the limiting deflection criteria. The loading type on the model is considered at the free end (tip).

Assumptions made are:

- The model is fixed at one end, considering the whole length of the model
- The links are uniform, made from the same material with the same thickness and depth.
- Gravity is considered to influence the model.
- The model is unactuated and vertical deflection is considered, ignoring horizontal deflections.

First, to get the maximum deflection of a loaded cantilever beam at the free end, Equation (1) is applicable derived from the loaded cantilever beam at free end shown in figure 2. $\boldsymbol{\delta_{max}} = \frac{\boldsymbol{Pl^3}}{\boldsymbol{3EI}}$ (2)

$\boldsymbol{\delta_{max}}$ - maximum deflection (m, mm)
P - concentrated point load (N)
l - Span length of the beam (m)
E - modulus of elasticity (Pa)

$\boldsymbol{I}$ **- the** Moment of Inertia (m^4)
y - axis in the y-direction on the beam
x - axis in the x-direction on the beam
for a standard cantilever beam shown in figure 2. Equation 1 displays the proportionality of load and deflection.

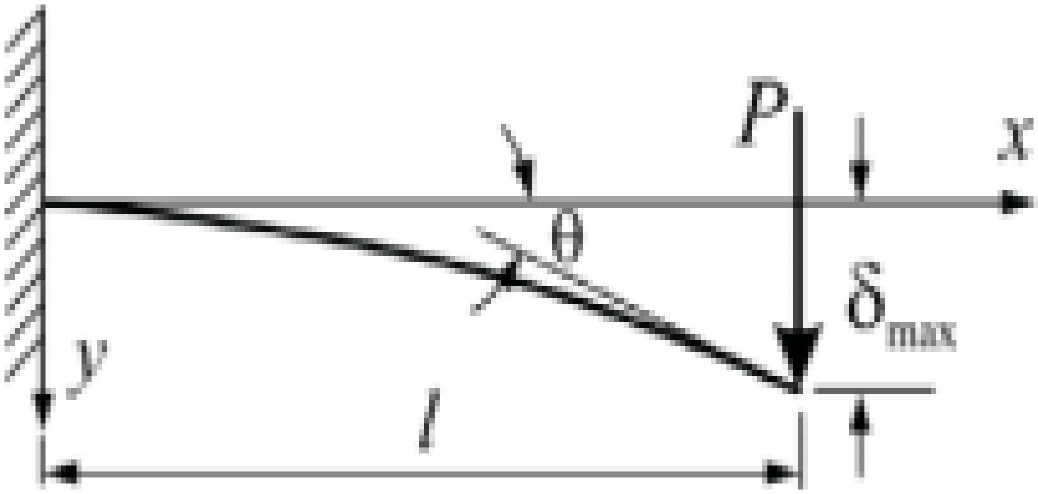

Figure 2: Cantilever Beam-Concentrated load ***P***, at the free end

In Mechanics of material (Anon., n.d.) to determine the allowable deflection ($\Delta_{\boldsymbol{allawable}}$), this two limiting criteria are applicable shown in table 2

Table 2: Allowable deflections.

Loading Type	Allowable deflection ($\Delta_{\boldsymbol{allawable}}$)
Live load	$\frac{l}{360}$
Dead load +live load	$\frac{l}{240}$
L is the span of the beam	

As the effect of gravity is taken into consideration the loading type (Dead +live load) is considered to determine the allowable deflection of the model. From the model, the span of the considered beam from the fixed point is 460 mm, therefore allowable deflection is derived.

$$Allowable\ deflection\ (\Delta_{\boldsymbol{allawable}}) = \frac{\boldsymbol{l}}{\boldsymbol{240}}$$
$$= \frac{\boldsymbol{460 \times 10^{-3}}}{\boldsymbol{240}}$$
$$Allowable\ deflection\ (\Delta_{\boldsymbol{allawable}}) = \boldsymbol{0.00192\ m}$$

The limiting deflection value is set to $\boldsymbol{1.92\ mm}$, with the set of values to be loaded at the tip the deflection that they will impose must not exceed this allowable deflection value.

2.3. Payloads selection

From the review of studies set of payloads to be used in simulations are selected from 0 to 50 N. With most of the two-link flexible manipulators both theoretical and experimental studies use nominal payloads ranging from 50g to 200g. The model is loaded with different payloads to find the maximum load that it can carry, and the limit is set at the maximum payload.

3. Simulations

(Afolabi, et al., 2019) describes that in engineering materials to increase the performance of a component and to prevent sudden failure it is significant to determine the failure of a component. Conducting simulations on a model helps to determine whether the model designed can be produced or applied by assessing the populated results. The model designed described in figure 1 was exported to the assembly environment on the Inventor software and a simulation study was created for stress analysis (FEA). With the Design objective of a single point and a study type of static analysis bonded type, a tolerance of 0.1mm for contacts set and before conducting simulation on the model first some parameters needed to be defined.

a) Material assigning: each component of the model is assigned with specific material type to what is to be in actual /practical. For simulation, the software can simulate a model with specified material to populate stresses and displacements results, modifying the material and geometry of the model was conducted with the Inventor software.
b) Constraints: For this study model as described that is a cantilever configuration, a fixed constraint type was done on one side of the model on the support rib as it is the fixed wall of the model.
c) Loads: This section was specifying the loads that will be exerted on the model, the loading criteria were done, considering the acceleration of gravity of $9.81 m/s^2$ in the x-direction (downwards) and from the lowest load to the least. The tip face was selected as is to where the payload is attached, then the force in x-direction (Fx) vector component was computed following the assumptions of vertical considerations.
d) Contacts: In the geometry, all contacts were generated automatically with the aid of the software computed easily. Inventor software provides types of contacts, with this model geometry the bonded type contacts were populated under the contact tree. This included parts which are bolted and where welding or glueing is to be applied.
e) Meshing: Meshing of a model it helps to define accurate results of the simulation, and with smaller grading factor a more uniform mesh is produced. With smaller elements, the simulation takes time to produce results. Mesh view was computed on the model, all the components were selected for the mesh. The element size of 0.1 as default was inputted, and the minimum element size of 0.2 specifying the minimum distance between mesh nodes. A grading factor of 1.5 was defined to specify the maximum ratio of adjacent mesh edges for transitioning between coarse and fine regions. A maximum turn angle of 60 degrees was computed as to specify the number of arcs and to increase the number of elements on curvy areas.

Figure 3 shows the meshed model with the loading specified the gravity and point load at the free end. The mesh generated 943 401 nodes and 580 209 elements on the model.

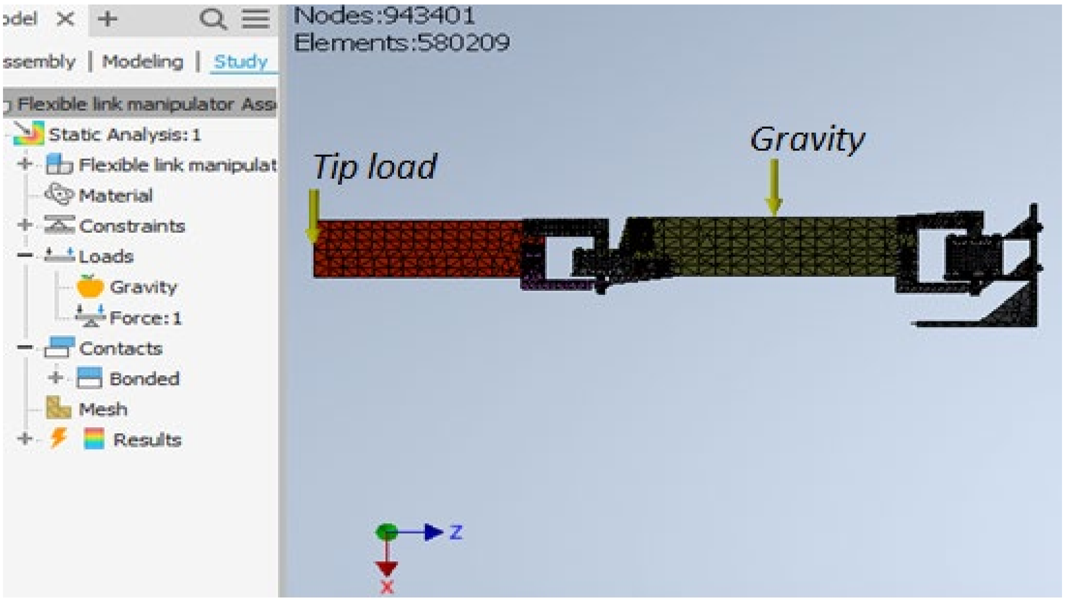

Figure 3: Meshed Model of FLM with load(s)

With all the parameters defined simulations were conducted and the computing of results displayed in the next section. The procedure followed for each load is repeated as from the first load, every after-simulation results were recorded and then changed loading values at the tip.

4. Results and Discussions

With the aid of the inventor software results were produced, Table 3 below shows the summary of the structural results produced by the analysis. The table and figures below display the results at failure load or the load which the model can be loaded to. It is noticed that the deflection occurred at the tip of the model, thus the area of stress concentration is on the second link.

Table 3: Summary of results produced at 32,5 N.

Name	Minimum	Maximum
Volume	$179325\ mm^3$	
Mass	$0{,}836908\ kg$	
Von Mises Stress	$0{,}00685473\ MPa$	$1229{,}92\ MPa$
1st Principal Stress	$-389{,}408\ MPa$	$1342{,}71\ MPa$
3rd Principal Stress	$-1596{,}85\ MPa$	$321{,}48\ MPa$
Displacement	$0\ mm$	$1{,}88978\ mm$
Safety Factor	$0{,}168303\ ul$	$15\ ul$

The results produced in table 3 shows that at load **32,5N** the maximum Von Mises stress was found to be $\mathbf{1229,92\ MPa}$, the first principal stress found is $\mathbf{1342,71\ MPa}$ and the third principal stress is $\mathbf{321,48\ MPa}$. The maximum displacement was found to be $\mathbf{1,88978\ mm}$, this value shows that the model cannot be loaded past the **32,5N** as the allowable deflection was set to approximately **1,91 mm**, therefore the model will fail when subjected to any load exceeding **32,5N**. The safety factor resulted to be **15 ul**.

In **Figure 4** below the simulation results at load **32,5 N** are shown and the section bar on each figure on the left side shows the yielded results from minimum (blue colour) to maximum (red colour), **Figure 4 (a)** displays the Von Mises stresses where the red colour on the bar represents the maximum value and the blue colour represents the minimum value. As in **figure 4 (b)** the first principal stresses are represented, **Figure 4 (c)** gives the third principal stresses and the area where the stresses are yielded are shown on the figures. **Figure 4 (d**) shows the results of the displacement yielded; the maximum displacement is found where the concentration of load subjected. On the model, at the free end of the link, the maximum deflection is exerted shown in red and the minimum deflection is shown in blue on the model in **figure 4 (d)**. In **figure 4 (e)** the maximum and minimum safety factor is shown, it is shown on the model where the safety factors are. Even the model is more stressed to the limiting deflection, it still shows the stability of withstanding the load which is subjected to.

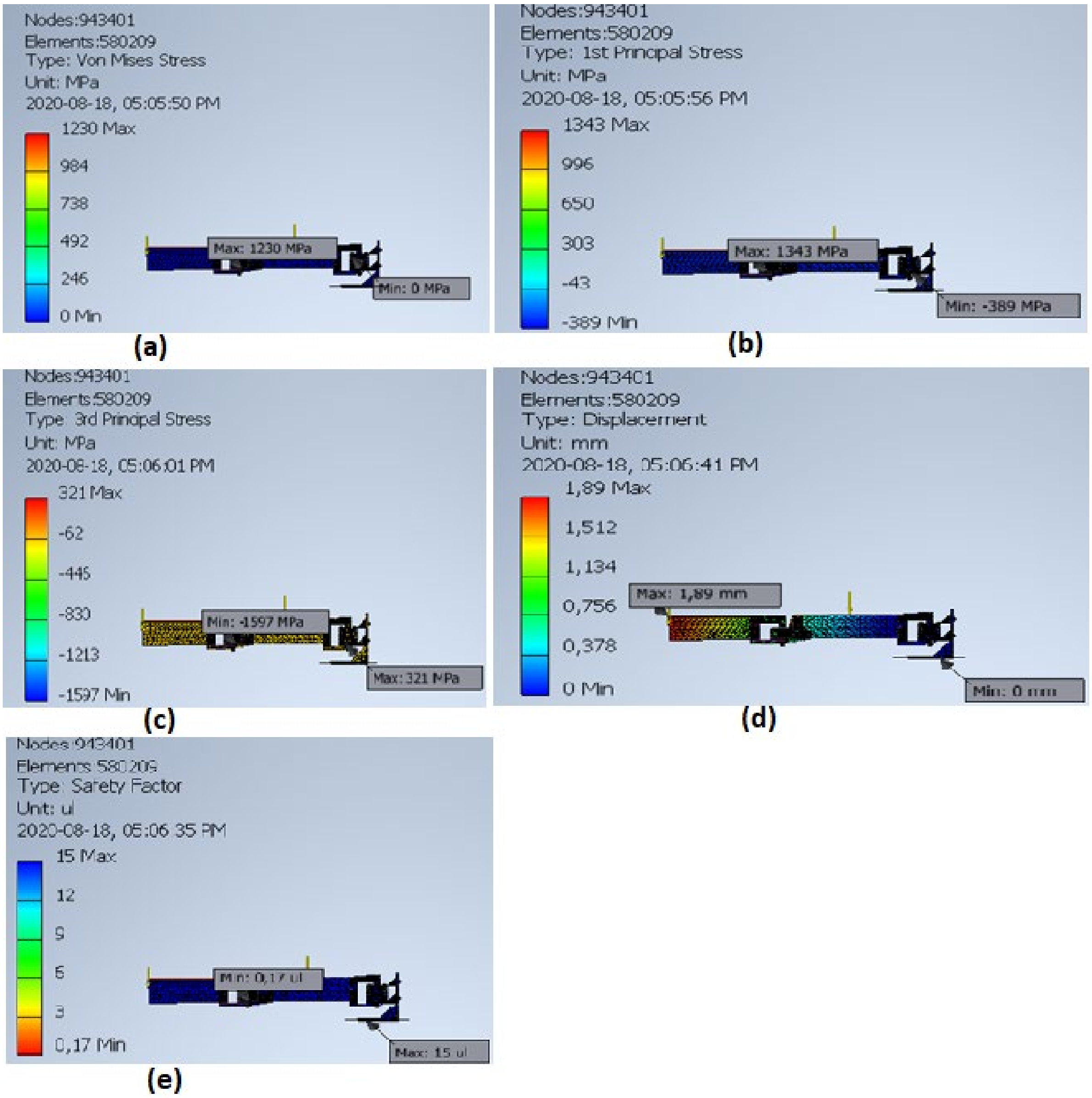

Figure 4:Simulation results at 32,5N load

The summary of results produced by the set of varying loads are tabulated below, the results show that when the loading at the tip is increased the Von Mises stress increases, first and third principal stresses increases. The results show the proportionality of loads and deflections, as the loading criteria increase the more the model deflects. It is shown that the model can be subjected to the limiting load of 32,5 N, where the allowable deflection is approximately equalled to that of simulation deflection at 32,5N. The Von Mises stresses produced at load 40 N is 1501,13 MPa and the first principal stress is found to be 1638,85 MPa, the deflection of the model is found to be 2,30621 mm which shows that it has exceeded the limiting deflection value. The maximum safety factor produced is 15 ul, this shows how safe it is to build and operate the model. A summary of applied varying payloads at at the tip of the model are shown in in table 4.

Table 4: Summary of simulation results at varying payloads.

Load (N)	Von Mises stress (MPa)	1rst Principal stress (MPa)	3rd Principal Stress (MPa)	Displacement/deflection (mm)	Safety factor (ul)
10	416,324	454,481	110,718	0,64050	15
20	777,923	849,245	04,389	1,19574	15
30	1139,48	1243,95	298,05	1,75096	15
32,5	1229,92	1342,71	321,48	1,88978	15
40	1501,13	1638,85	391,723	2,30621	15

With the set of values used at the tip of the model. The table 5 below shows the maximum deflection produced at each set of payloads the model was subjected to. The Youngs modulus (E) for the aluminium is **68,9 GPa** and the Moment of Inertia (I) is $\mathbf{3,125 \times 10^{-8}\ m^4}$**.** The calculated flexural rigidity (EI) is 2153,125. Therefore, the results for theoretically maximum deflection was calculated from equation 1 below then tabulated the numerical results below in Table 5.

$$\boldsymbol{\delta_{max}} = \frac{\mathbf{(10)(0,46)^3}}{\mathbf{3(2153,125)}}$$
$$= \mathbf{0,15069\ mm}$$

Table 5: Numerical results of maximum deflection with varying payloads

Load (N)	Maximum deflection ($\boldsymbol{\delta_{max}}$) (mm)
10	0,15069
20	0,3014
30	0,4521
32,5	0,4897
40	0,6028

It is seen from the calculated results that the maximum deflections are very small when the model is subjected to payloads. Looking at payload 32,5 N which was found to be a failure load in simulation results, but from the theoretical results, the maximum deflection is 0,4897 mm. A major difference is found to be there when comparing the results.

Graph of the simulated results and calculated results are shown in figure 5 below, from simulations the model appears to deflect drastically under loading. Theoretically, the model was having a slight deflection when subjected to load(s) at the tip. The cause or error in differing results might have caused by considering the links to be truncated to one link in theoretical calculations, as the hub joint with openings were not accounted in the calculations. It shows that when using a modelling tool to assess a design it provides an ideal system results to the actual world model.

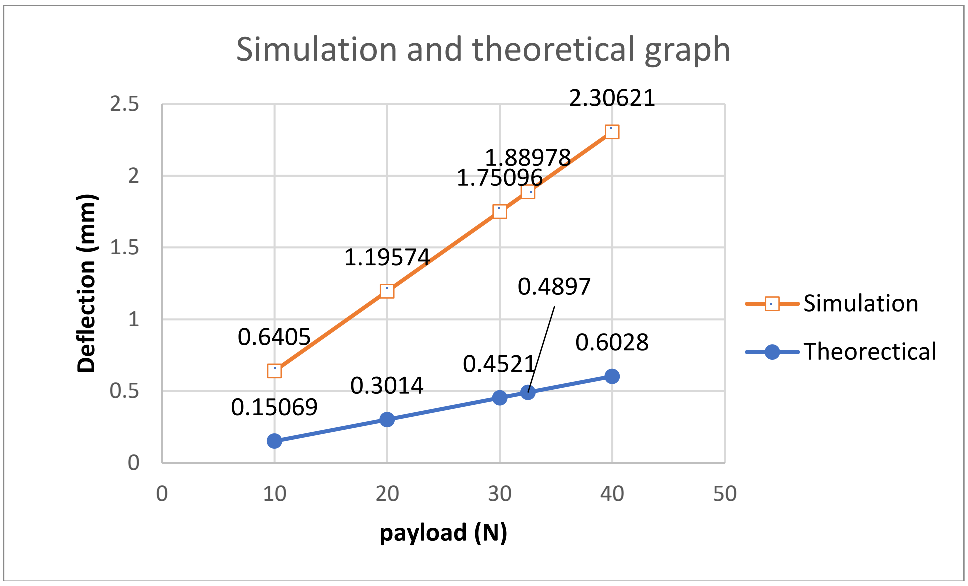

Figure 5: Graph of simulated results and theoretical (calculated)

Is shown on the graph above figure 5 that when the loading is increased the more the model deflects, the deflection of the model increases linearly with the load. It shows that the more the model is subjected to loading it will bend until it fails. The loading criteria used in this study shows the weight ratio theory mostly discussed in flexible manipulators studies, as it is shown that as light as it is designed it can carry high loads. It is seen that the results follow the stress-strain graph, that the higher the stress the higher the strain.

It is seen that having a light model reduces the weight of the system, with aluminium selected as a material type for the design. The model proved to carry the load at the tip as light as it is without failing at low payloads. This type of design model can reduce the cost of operation in the manufacturing industry, and reduction of power usage, because of having a lighter system the lower the cost in operation.

5. Conclusions

In this paper a study was carried out to validate the stability of a designed two link Flexible manipulator, the aim was to assess to what load it can hold to the allowable deflection. A limiting deflection value of 1,91mm was derived and a set of varying payloads were subjected at the tip of the model. With the help of Inventor software, finite element analysis (FEA) was carried out to simulate the set of varying payloads. It was found that at the load that can be withstood by the model is 32,5 N the deflection is 1,8898 mm which is approximately equals to allowable deflections, the von mises stress of 1229,92 MPa was produced, first principal stress found was 1342,71 MPa, third principal stress of 321,48 MPa and a maximum safety factor of 15 ul. It was seen from the results that the increase of varying loads the more the model deflects. It can be concluded that the aim of assessing the model stability was achieved, the model cannot be subjected to loads more than 32,5 N and the model is advantageous as it carries more load to its weight ratio. It can help reduce operation cost in the manufacturing industry as it was seen from the simulated results. Future studies can be carried out with a physical system actuated.

6. References

[1] Afolabi, S. O. et al., 2019. Design and finite element analysis of a fatigue life prediction for safe and economical machine shaft. *Journal of Materials Research and Technology,* March, 8(1), pp. 105-111.

[2] Afolabi, S. O. et al., 2019. Design and finite element analysis of a fatigue life prediction for safe and economical machine shaft. *Journal of Materials Research and Technology,* 8(1), pp. 105-111.

[3] Agee, J. T., Bingul, Z. & Kizir, S., 2014. Tip trajectory control of a flexible-link manipulator using an intelligent proportional-integral (iPI) controller. *Transactions of the Institute of Measurement and Control,* 24 January, 36(4), p. 673–682.

[4] Ahmad, M. A., Mohamed, Z. & Hambali, N., 2008. *Dynamic modelling of a two-link flexible manipulator system incorporating payload.* Singapore, IEEE, pp. 96-101.

[5] Anon., n.d. *learncivilengineering.* [Online]
Available at: http://www.learncivilengineering.com/wp-content/uploads/2014/06/Deflection.pdf
[Accessed 20 July 2020].

[6] Bhandari, R. & Kalaichelvi, V., 2017. *Analysis and control techniques for a two-link underactuated manipulator.* Salmabad, IEEE, pp. 1-5.

[7] Durbaca, I. et al., 2019. Approaches looking at finite element analysis of a structural model of lid stratified with cellular polymeric core specific to a pressure vessel. *Materiale Plastice,* 56(1), pp. 156-162.

[8] Gao, H., He, W., Zhou, C. & Sun, C., 2019. Neural Network Control of a Two-Link Flexible Robotic Manipulator Using Assumed Mode Method. *IEEE TRANSACTIONS ON INDUSTRIAL INFORMATICS,* February, 15(2), pp. 755-765.

[9] Lochan, K., Singh, J. P., Roy, B. K. & Subudhi, B., 2018. Hidden Chaotic Path Planning and Control of a Two-Link Flexible Robot Manipulator. In: V. Pham, S. Vaidyanathan, C. Volos & T. Kapitaniak, eds. *Nonlinear Dynamical Systems with Self-Excited and Hidden Attractors. Studies in Systems, Decision and Control.* s.l.: Springer, Cham, pp. 433-463.

[10]Mustika, V., Triono, A. & Wibowo, R. K. K., 2020. Process simulation of power screw failure on fatigue load using Autodesk inventor. *Journal of Physics: Conference Series,* 1465(1), pp. 1-9.

[11]Pedram, M. & Khedmati, M. R., 2014. The effect of welding on the strength of aluminium stiffened plates subject to combined uniaxial compression and lateral pressure. *International Journal of Naval Architecture and Ocean Engineering,* March, 6(1), pp. 39-59.

[12]Pradhan, S. K. & Subudh, B., 2013. *Fuzzy learning-based adaptive control for a two-link flexible manipulator.* Hyderabad, IEEE, pp. 282-287.

[13]Pradhan, S. K. & Subudhi, B., 2011. *NARMAX modelling of a two-link flexible robot.* Hyderabad, IEEE, pp. 1-5.

[14]Rezaei, V. & Shafei, A., 2019. Dynamic Analysis of Flexible Robotic Manipulators Constructed of Functionally Graded Materials. *Iranian Journal of Science and Technology - Transactions of Mechanical Engineering,* 1 07, Volume 43, pp. 327-342.

[15]Sahu, U. K., Patra, D. & Subudhi, B., 2017. *Network-based control of 2-DOF serial flexible link manipulator.* Penang, Malaysia, IEEE, pp. 333 - 338.

[16]Ying, . S. & Wenkai, C., 2008. *Particle filter applied to a manipulator with two flexible links.* Kunming, China, IEEE, pp. 705 - 708.

[17]Yu, Y., Yuan, Y., Fan, X. & Yang, H., 2015. *Back-stepping control of two-link flexible manipulator based on extended state observer.* Hangzhou, IEEE, pp. 846-849.

[18]Zuyev, A. L., 2015. Observer-Based Stabilization of a Manipulator Based on the Timoshenko Beam Model. In: Cham, ed. *Partial Stabilization and Control of Distributed Parameter Systems with Elastic Elements. Lecture Notes in Control and Information Sciences.* Donetsk Ukraine: Springer, pp. 131-167.

7. Biographies

Xichabo Sheriff Nyathi is currently a Master of Technology student in engineering at the University of Johannesburg (2020). He has earned his Bachelor of Technology (Btech) in mechanical engineering and National Diploma (NDip) in mechanical engineering from the University of Johannesburg. He is a Lecturer at Central Johannesburg College in engineering science and mathematics department. He has worked with Resolution Circle Pty Ltd, a training institution in fitting and turning, boiler making, basic electrical and electronics, automation, and commercial projects. He was a tutoring member at the University of Johannesburg. His research interest is in robotics, design, modelling, and manufacturing.

FK Tekweme is a senior lecturer in the Department of Mechanical Engineering at the University of Johannesburg, RSA. He holds a BEng in Mechanical Engineering from the University of Kinshasa, Masters, and Ding from the University of Johannesburg, RSA. Francis's research interests include Microwave energy heating and Robotics, Artificial Intelligence (Machine Learning), and Programming.